Hybrid IE-DDM-MLFMA with Gauss-Seidel Iterative Technique for Scattering from Conducting Body of Translation

Ming Jiang, Jun Hu, Ran Zhao, Xiang Wei, and Zai-ping Nie

School of Electronic Engineering
University of Electronic Science and Technology of China, Chengdu 611731, People's Republic of China
hujun@uestc.edu.cn

Abstract ─ In this paper, a hybrid Integral Equation-Domain Decomposition Method-Multilevel Fast Multipole Algorithm (IE-DDM-MLFMA) with Gauss-Seidel iterative technique is proposed to calculate the scattering from perfectly electric conducting Body of Translation (BoT). The BoT can be partitioned into translational non-overlapping sub-domains. A hybrid local/global MLFMA framework is adopted to realize efficient matrix-vector multiplication in sub-domains and between sub-domains by utilizing the feature of translational invariance of BoT. To reduce the number of interactions between sub-domains, Gaussian-Seidel iterative technique is applied. Numerical examples are presented to demonstrate the efficiency of the present method.

Index Terms ─ Body of translation, Gauss-Seidel iteration, multilevel fast multipole algorithm, non-overlapping domain decomposition method.

I. INTRODUCTION

In practical electronic information area, some important conducting objects have gained intensive interests and attention of researchers in electromagnetic community, which are Bodies of Translation (BoT). In practice, high speed trains, aircraft wings and fuselages can often be approximated as bodies of translation. Some numerical methods including the method of moment have been developed to solve the BoT. Medgyesi-Mitschg and Putnam developed a general systematic approach based on the method of moment for BoT in 1983. The functional variation of the surface currents along the axis of translation of the BoT is represented by a total-domain Fourier expansion and a piecewise continuous function along the generating curve [1].

To solve electromagnetic problems for large BoT, Davis used the rectangular basis functions to segment the body of translation into a set of identical cells along the translation of the body. The impedance matrix can be evaluated efficiently by converting all surface integrals over the basis functions into line integrals [2]. Medgyesi-Mitschg and Putnam also expand the method of moment for analysis of wire antenna attached on the BoT by incorporating a special junction basis function set for the antenna attachment points [3]. Although the above methods can accurately solve the BoT problems, they can be only applicable for moderate problems due to large computational complexity of method of moment. As a well-known fast algorithm used for integral equation, Multilevel Fast Multipole Algorithm (MLFMA) [4] has only computational complexity of O(NlogN). Although MLFMA is a general fast algorithm for accelerating matrix vector multiplication in iterative solution of matrix equation for objects with arbitrary geometry, for very large BoT problems, the MLFMA is still time consuming and requires large memory storage. Thus, it is still necessary to seek novel numerical methods to solve larger BoT problems more efficiently.

In order to realize efficient solution of conducting structures with large sizes, the Multi-Region Iterative Multilevel Fast Multipole Algorithm (MRI-MLFMA) combined the Generalized Forward/Backward (GFB) technique was developed by us [5]. Although it has better performance than traditional MLFMA, the buffer zones are required to ensure the continuity of current across the interfaces between multi-regions, and the property of matrix can't be improved in

Submitted On: September 1, 2013
Accepted On: September 26, 2014

essence. Recently, a novel Integral Equation based non-overlapped Domain Decomposition Method (IE-DDM) [6] is introduced by Peng, et al. In this paper, in order to realize efficient solution of scattering from the Perfect Electric Conductor (PEC) BoT with large electric size, a hybrid scheme named IE-DDM-MLFMA with Gaussian-Seidel iterative technique is developed. The computational BoT is partitioned into several same closed sub-domains, so Combined Field Integral Equation (CFIE) can be used in each sub-domain. In addition, Gauss-Seidel iterative technique is used to update the unknown current in each sub-domain in real time. A hybrid local/global MLFMA framework is adopted to realize efficient matrix-vector multiplication in sub-domains and between sub-domains by utilizing translation invariant feature of BoT.

The rest of paper includes the following parts. Section II gives a brief introduction on integral equation based domain decomposition method, followed by Section III for the extension of IE-DDM for the BoT. Section IV presents some typical numerical results, and finally, the conclusions are given in Section V.

II. INTEGRAL EQUATION BASED DOMAIN DECOMPOSITION METHOD

A. Equation formatting boundary value statement

Considering electromagnetic scattering by a PEC target occupying a finite domain illustrated in Fig. 1. The scattered electric and magnetic fields in free space can be obtained from the Stratton-Chu representation formula [7,8] as:

$$\boldsymbol{E}^s(\boldsymbol{J};\partial\Omega)(\boldsymbol{r}) = \eta_0 \boldsymbol{L}_{k_0}(\boldsymbol{J};\partial\Omega)(\boldsymbol{r}) \quad \boldsymbol{r}\in\Omega_{ext}, \tag{1}$$

$$\boldsymbol{H}^s(\boldsymbol{J};\partial\Omega)(\boldsymbol{r}) = K_{k_0}(\boldsymbol{J};\partial\Omega)(\boldsymbol{r}) \quad \boldsymbol{r}\in\Omega_{ext}, \tag{2}$$

where η_0 is the free space intrinsic impedance and k_0 is the free space wave number. $\boldsymbol{J}$ is electric current on the surface $\partial\Omega$. The Electric Field Integral Operator (EFIO) and Magnetic Field Integral Operator (MFIO) are denoted by L and K as follows:

$$L_{k_0}\left(\boldsymbol{X}(\boldsymbol{r}');\partial\Omega\right)(r) = ik_0\int_{\partial\Omega}\boldsymbol{X}(\boldsymbol{r}')G(\boldsymbol{r},\boldsymbol{r}';k_0)d\boldsymbol{r}' + \frac{i}{k_0}\int_{\partial\Omega}\left(\nabla'\bullet\boldsymbol{X}(\boldsymbol{r}')\right)\nabla G(\boldsymbol{r},\boldsymbol{r}';k_0)d\boldsymbol{r}'$$

$$K_{k_0}\left(\boldsymbol{X}(\boldsymbol{r}');\partial\Omega\right)(r) = \int_{\partial\Omega}\nabla G(\boldsymbol{r},\boldsymbol{r}';k_0)\times\boldsymbol{X}(\boldsymbol{r}')d\boldsymbol{r}', \tag{3}$$

$G(\boldsymbol{r},\boldsymbol{r}';k_0) = \dfrac{\exp(ik_0|\boldsymbol{r}-\boldsymbol{r}'|)}{4\pi|\boldsymbol{r}-\boldsymbol{r}'|}$ is the Green's function in free space.

Here, the following tangential trace and twisted tangential trace operators will be used [9,10]:

$$\pi_\tau\left(v_m\right) := \hat{\boldsymbol{n}}_m\times\left(\boldsymbol{v}_m\times\hat{\boldsymbol{n}}_m\right)\big|_{\partial\Omega_m}\ \gamma_\tau\left(v_m\right) := \hat{\boldsymbol{n}}_m\times\boldsymbol{v}_m\big|_{\partial\Omega_m}. \tag{4}$$

So Eq. (1), (2) can be rewritten:

$$\boldsymbol{e}^s(\boldsymbol{j};\partial\Omega)(\boldsymbol{r}) = \pi_\tau\boldsymbol{L}_{k_0}(\boldsymbol{j};\partial\Omega)(\boldsymbol{r}) \quad \boldsymbol{r}\in\partial\Omega, \tag{5}$$

$$\boldsymbol{j}^s(\boldsymbol{j};\partial\Omega)(\boldsymbol{r}) = \frac{1}{2}\boldsymbol{j} + \gamma_\tau\bar{K}_{k_0}(\boldsymbol{j};\partial\Omega)(\boldsymbol{r}) \quad \boldsymbol{r}\in\partial\Omega, \tag{6}$$

where $\bar{K}$ stands for the principle value of K.

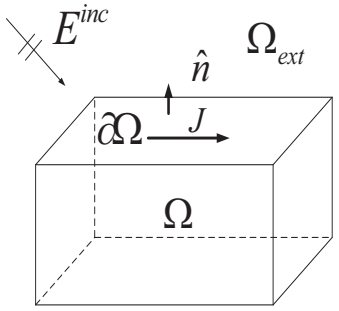

Fig. 1. EM wave scatting by PEC.

B. Decomposed combined field integral equations

The current integral equation based on domain decomposition method begins by partitioning the original problem domain into N non-overlapping sub-domains:

$$\Omega = \bigcup_{i=1,N}\Omega_i,\ \Omega_i\bigcap\Omega_j = \varnothing,\ \ 1\le i\ne j\le N. \tag{7}$$

Denote the boundary of Ω_i as $\partial\Omega_i$, the touching face Γ_{ij} is defined as $\Gamma_{ij} = \partial\Omega_i\bigcap\partial\Omega_j$. Obviously, $\Gamma_{ij} = \Gamma_{ji}$; however, here we still make an artificial distinction in order to the possibility of differing triangulations on either side of the touching face. Γ_{ij} is used when Ω_i is the "master" sub-domain and Γ_{ji} if the converse is true. Moreover, the boundary $\partial\Omega_i$ contains two parts $\partial\Omega_i = \partial\widehat{\Omega}_i\bigcup\Gamma_{ij}, \partial\widehat{\Omega}_i = \partial\Omega_i/\Gamma_{ij}$. The reason we do so is due to the fact that the touching face meshes on Γ_{ij} and Γ_{ji} are allowed to be non-matching grids (non-conformal). For the sake of simplicity and without loss of generality, here we consider

only the case of $N=2$, as shown in Fig. 2. Subsequently, the well-known Combined Field Integral Equation (CFIE) governing the electric and magnetic fields on the PEC surface $\partial\Omega_1$ and $\partial\Omega_2$, is written as follows, respectively:

$$(1-\alpha)\boldsymbol{j}_i(\boldsymbol{r})-\alpha\boldsymbol{e}_i^s(\boldsymbol{r})-(1-\alpha)\boldsymbol{j}_i^s(\boldsymbol{r}) = \alpha\boldsymbol{e}_i^{INC}(\boldsymbol{r})+(1-\alpha)\boldsymbol{j}_i^{INC}(\boldsymbol{r}) \quad (i=1,2), \tag{8}$$

where $\boldsymbol{j}_i^{INC}(\boldsymbol{r})=\eta_0\gamma_\tau\left(H_i^{INC}(\bar{r})\right), \boldsymbol{e}_i^{INC}(\boldsymbol{r})=\pi_\tau\left(E_i^{INC}(\bar{r})\right)$ and α is the factor of CFIE.

Taking the sub-domain Ω_1 for example, note that the incident field on the $\partial\Omega_1$ can be written as follows:

$$\boldsymbol{e}_1^{INC}(\boldsymbol{r})=\boldsymbol{e}_1^{inc}(\boldsymbol{r})+\boldsymbol{e}_2^s(\boldsymbol{r}) \qquad \boldsymbol{r}\in\partial\Omega_1, \tag{9}$$

$$\boldsymbol{j}_1^{INC}(\boldsymbol{r})=\boldsymbol{j}_1^{inc}(\boldsymbol{r})+\boldsymbol{j}_2^s(\boldsymbol{r}) \qquad \boldsymbol{r}\in\partial\Omega_1. \tag{10}$$

The first term in Eq. (9-10) stands for the primary incident field, the second term stands for the scattering field excited by the sources on the $\partial\Omega_2$. Straightforwardly, the combining of (8), (9) and (10) results in the CFIE solver for the decomposed problem.

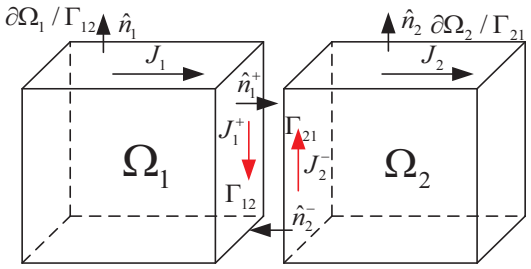

Fig. 2. Non-overlapping IE-DDM scheme: 2 sub-domains.

C. Transmission conditions

The decomposed problem will not be equivalent to the original entire domain problem unless proper transmission conditions are observed for every sub-domain touching face Γ_{ij}. Obviously, the transmission condition $\boldsymbol{J}_1^+=-\boldsymbol{J}_2^-$ should be satisfied on the touching faces. So the following Robin transmission condition on Γ_{12}, Γ_{21} are used [10]:

$$\alpha\boldsymbol{e}_1^{INC}(\boldsymbol{r})\big|_{\Gamma_{12}}+(1-\alpha)\boldsymbol{j}_1^{INC}(\boldsymbol{r})\big|_{\Gamma_{12}} = -\alpha\boldsymbol{e}_1^s(\boldsymbol{r})\big|_{\Gamma_{12}}-(1-\alpha)\boldsymbol{j}_2^-(\boldsymbol{r})\big|_{\Gamma_{21}}-(1-\alpha)\boldsymbol{j}_1^s(\boldsymbol{r})\big|_{\Gamma_{12}}, \tag{11}$$

$$\alpha\boldsymbol{e}_2^{INC}(\boldsymbol{r})\big|_{\Gamma_{21}}+(1-\alpha)\boldsymbol{j}_2^{INC}(\boldsymbol{r})\big|_{\Gamma_{21}} = -\alpha\boldsymbol{e}_2^s(\boldsymbol{r})\big|_{\Gamma_{21}}-(1-\alpha)\boldsymbol{j}_1^+(\boldsymbol{r})\big|_{\Gamma_{12}}-(1-\alpha)\boldsymbol{j}_2^s(\boldsymbol{r})\big|_{\Gamma_{21}}. \tag{12}$$

To expand the surface current in each sub-domain, traditional RWG basis function [11] is used. To assure the current continuity across corner edges, a corner edge based RWG basis function is defined for corner edge current. It not only avoids the introducing of half RWG basis function, but keeps exactly the same formulation of the CFIE matrix with the one of single sub-domain. A demonstrative figure is shown in Fig. 3.

Considering the coefficient vector $\boldsymbol{x}_i=\left[\boldsymbol{x}_i^e \quad \boldsymbol{x}_i^c \quad \boldsymbol{x}_i^t\right]^T$, stands for the coefficients of the RWG basis function for current on exterior surface, on the corner edge and on the touching face respectively.

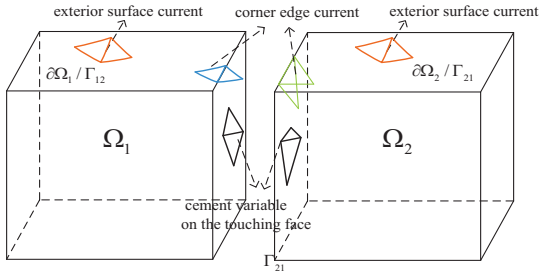

Fig. 3. Three kinds of RWG basis functions for expanding the current on exterior surface, on the corner edge and on the touching face in the IE-DDM.

Based on Galerkin testing, we yield the matrix equation of IE-DDM as follows:

$$\begin{bmatrix}\boldsymbol{A}_1 & 0\\ 0 & \boldsymbol{A}_2\end{bmatrix}\begin{bmatrix}\boldsymbol{x}_1\\ \boldsymbol{x}_2\end{bmatrix}=\begin{bmatrix}\boldsymbol{b}_1\\ \boldsymbol{b}_2\end{bmatrix} + \begin{bmatrix}\boldsymbol{B}_1 & \boldsymbol{C}_{12}\\ \boldsymbol{C}_{21} & \boldsymbol{B}_2\end{bmatrix}\begin{bmatrix}\boldsymbol{x}_1\\ \boldsymbol{x}_2\end{bmatrix}+\begin{bmatrix}0 & \boldsymbol{D}_{12}\\ \boldsymbol{D}_{21} & 0\end{bmatrix}\begin{bmatrix}\boldsymbol{x}_1\\ \boldsymbol{x}_2\end{bmatrix}, \tag{13}$$

where

$$\boldsymbol{A}_i=\begin{bmatrix}\boldsymbol{A}_i^{ee} & \boldsymbol{A}_i^{ec} & \boldsymbol{A}_i^{et}\\ \boldsymbol{A}_i^{ce} & \boldsymbol{A}_i^{cc} & \boldsymbol{A}_i^{ct}\\ \boldsymbol{A}_i^{te} & \boldsymbol{A}_i^{tc} & \boldsymbol{A}_i^{tt}\end{bmatrix}, \boldsymbol{B}_i=\begin{bmatrix}0 & 0 & 0\\ \boldsymbol{B}_i^{ce} & \boldsymbol{B}_i^{cc} & \boldsymbol{B}_i^{ct}\\ \boldsymbol{B}_i^{te} & \boldsymbol{B}_i^{tc} & \boldsymbol{B}_i^{tt}\end{bmatrix},$$

$$\boldsymbol{C}_{ij}=\begin{bmatrix}\boldsymbol{C}_{ij}^{ee} & \boldsymbol{C}_{ij}^{ec} & \boldsymbol{C}_{ij}^{et}\\ \boldsymbol{C}_{ij}^{ce} & \boldsymbol{C}_{ij}^{cc} & \boldsymbol{C}_{ij}^{ct}\\ 0 & 0 & 0\end{bmatrix}, \boldsymbol{D}_{ij}=\begin{bmatrix}0 & 0 & 0\\ 0 & 0 & 0\\ 0 & \boldsymbol{D}_{ij}^{tc} & \boldsymbol{D}_{ij}^{tt}\end{bmatrix}, \text{ and}$$

$1\le i\ne j\le 2$.

It is worth to note that two triangles of RWG basis function related to corner edges locate on different surfaces; i.e., exterior surface and touching face. So, different boundary conditions are used in corresponding triangle for this special RWG basis function. The matrix blocks $\boldsymbol{A}_i$ forms the usual Combined Field Integral Equation (CFIE) matrix for sub-domain Ω_i. The sub-matrix $\boldsymbol{B}_i$ denotes the self-impedance matrix of each sub-domain, the sub-matrix $\boldsymbol{C}_{ij}$ denotes mutual impedance matrix between two sub-domains, while the sub-matrix $\boldsymbol{D}_{ij}$ is sparse motar matrix.

III. GAUSS-SEIDEL ITERATION TECHNIQUE

For solution of Eq. (13), two iterative processes are needed: the inner iterative process and the outer iterative process. For the inner iterative process, GMRES iterative technique is used. For the outer iterative process, Gauss-Seidel iterative technique is used instead of Jacobi iteration technique in this paper; which updates the currents on each sub-domain in real time. The Gauss-Seidel iteration procedure is given as follows:

Step 1: Initialization

The currents in all N sub-domains are initialized to 0, starting the outer iteration, $k=1$.

Step 2: Iterative solution of sub-domains

For $i=1,2,...,N$ (N is the number of sub-domains):

a) The Eq. (13) is solved via GMRES iterative solver in each sub-domain;
b) Updating the current in sub-domain in real time once it has been solved.

Step 3: Error computation and convergence evaluation

Computing the maximal relative residual error, $\text{error\_max}(k)$, for N sub-domains. If the error achieves the desired threshold, the outer iteration process is over. Otherwise, $k=k+1$; return to Step 2, continue the iteration process.

The maximal relative residual error of current at the k-th outer iteration is defined as:

$$\text{error\_max}(k)=\max_i \frac{\left\|\boldsymbol{I}_i^k-\boldsymbol{I}_i^{k-1}\right\|}{\left\|\boldsymbol{I}_i^k\right\|}. \qquad (14)$$

$\boldsymbol{I}_i^k$ denotes the currents on the i-th sub-domain at the k-th outer iteration. $\|\ \|$ denotes the 2-norm of the complex vector.

IV. HYBRID LOCAL/GLOBAL MLFMA FRAMEWORK

For the problem of BoT, the computational original domain can be partitioned into several same sub-domains, as shown in Fig. 4. Because for each sub-domain, the self-coupling is the same, the self-impedance matrix in each sub-domain can be implemented only once. Here, hybrid local/global MLFMA framework is developed: local MLFMA is used to reduce the time of matrix filling and matrix-vector multiplication in each sub-domain, global MLFMA is used to accelerate the computation of coupling between sub-domains.

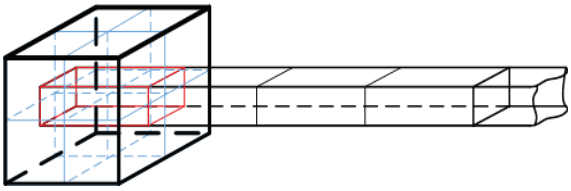

Fig. 4. Hybrid local/global MLFMA framework for BoT: each sub-domain is same.

From Eq. (13), we can see that there are three kinds of matrix blocks $\boldsymbol{A}$, $\boldsymbol{B}$, $\boldsymbol{C}$. For matrix $\boldsymbol{A}$, we can implement the matrix-vector multiplication of $\boldsymbol{A}\bullet x$; by local MLFMA, it is the same with traditional MLFMA because matrix $\boldsymbol{A}$ is exactly the same with traditional impedance matrix of sub-domain divided. For matrix $\boldsymbol{B}$, $\boldsymbol{C}$ are for specific sources and observation points, different from traditional case in which the sources distribution is identical with the observation points distribution.

To implement the MLFMA, the object is enclosed by a large cube which is partitioned into eight children cubes, every sub-cube is then recursively subdivided into smaller cubes until the edge length of the finest cube is about 0.3 wavelength. Further non-empty cubes are recorded using tree-structured data at all levels.

The representation of matrix-vector multiplication using MLFMA is often written as:

$$A\bullet x=A_{near}\bullet x+U^t\bullet T\bullet V\bullet x. \qquad (15)$$

The matrix A_{near} represents the interaction matrix from nearby region which is computed by

the MoM. V,T,U^t is aggregation, translation, disaggregation matrix respectively; they represent three processes of interaction between non-nearby regions. The details can be referred to references [4,12].

V. NUMERICAL RESULTS

This section validates the accuracy and demonstrates the efficiency through some numerical examples. To validate the accuracy of IE-DDM code developed here, two examples A1-A2 are given first. The examples B1-B3 are used to show the ability of the present method for the BoT.

A1. EM scattering from a PEC sphere

Bistatic RCS of a PEC sphere of radius R=3 m excited by a θ polarized plane wave incident from -z direction is computed. The frequency is f=300 MHz. The sphere is partitioned into two closed hemispheres. The conventional MLFMA and MIE method are used for comparisons. The number of unknowns by the MLFMA and IE-DDM-MLFMA is 49,531 and 55,401 respectively.

The RCS results by the MIE method and IE-DDM-MLFMA are shown in Fig. 5. A good agreement between the result by the IE-DDM-MLFMA and the one by MIE method is confirmed. Figure 6 shows the current distribution using the conventional MLFMA and IE-DDM-MLFMA respectively. They agree well with each other. In addition, the electric currents across the touching face between two neighbouring sub-domains are normal continuous.

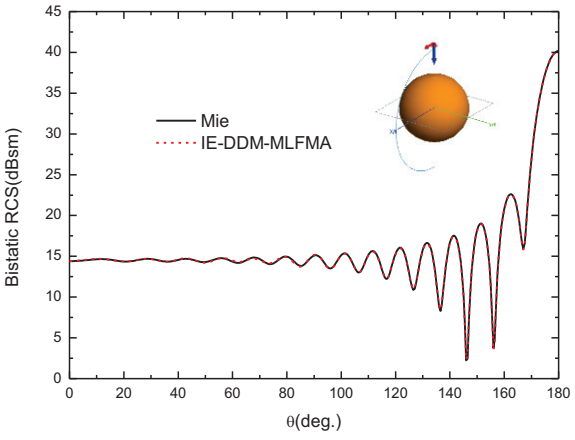

Fig. 5. Bistatic RCS of PEC sphere.

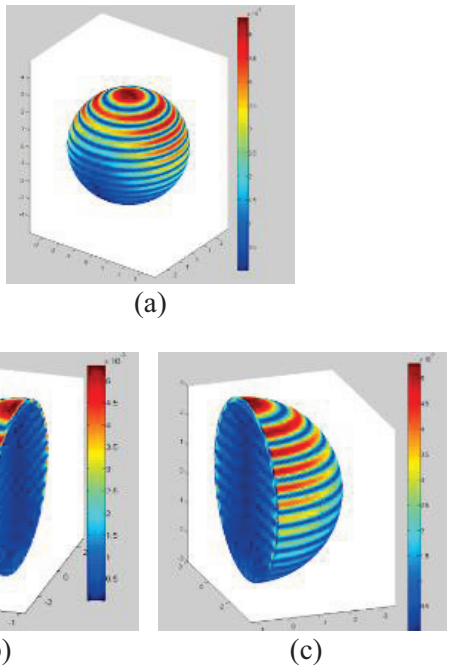

Fig. 6. (a) Current distribution of PEC sphere using conventional MLFMA, and (b), (c) current distribution of 2 sub-domains using IE-DDM-MLFMA.

A2. Simplified helicopter model

The second example we consider is a simplified helicopter model with length of 4.5 m. The entire model is divided into 8 closed-surface regions and different color denotes different regions, as depicted in Fig. 7. The frequency of the incident plane wave $(\theta_i = 90°, \varphi_i = 0°)$ is 3.0 GHz. Each region is meshed independently according to its geometry complexity. Due to the non-conformal feature of the IE-DDM, each sub-region can be meshed with good quality, which results in 461,667 totally. The bistatic RCS results with horizontal polarization in the $z-x$ plane are plotted in Fig. 8 (a), together with the MLFMA solutions. It is found that good agreements are obtained. In addition, IE-DDM converges to relative residual error of 10^{-2} with 7 outer iterations.

The bistatic RCS results by the MLFMA and the IE-DDM-MLFMA are shown in Fig. 8 (a), a very good agreement is achieved. The current distribution of Helicopter is also given in Fig. 8 (b).

The above two examples have validated the ability of the IE-DDM-MLFMA. In the following

parts, the examples B1-B3 are used to demonstrate the performance of the present method for BoT.

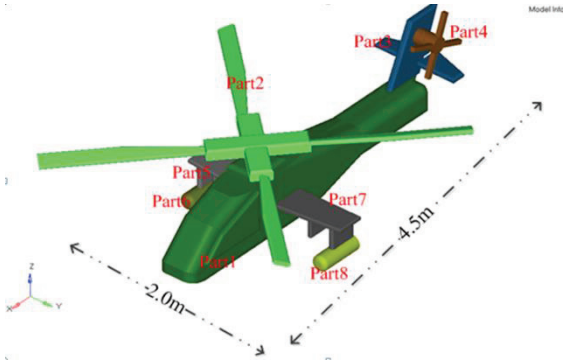

Fig. 7. Geometry model of simplified helicopter: 8 sub-domains.

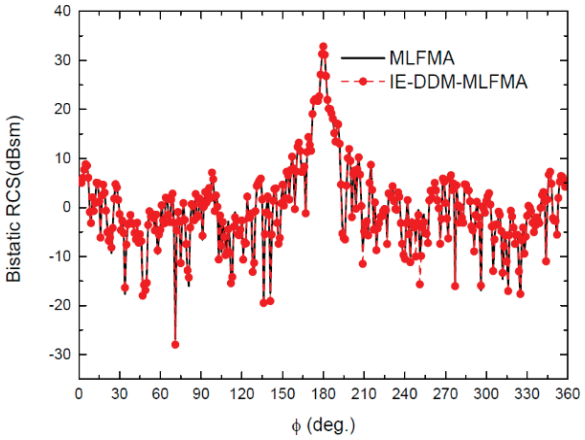

(a)

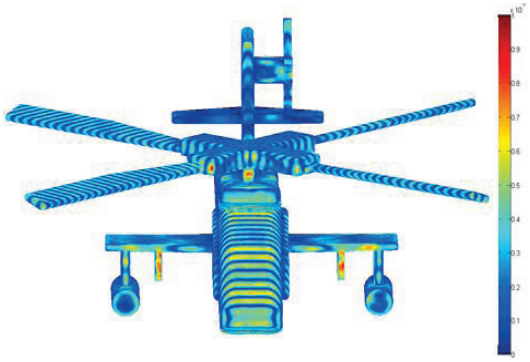

(b)

Fig. 8. (a) RCS of the helicopter model, and (b) current distribution of helicopter at 3 GHz.

B1. EM scattering from a PEC cylinder

A PEC cylinder of radius R=0.5 m and height H=1 m is excited by a plane wave incident from -z direction. The frequency is f=0.3 GHz. The cylinder is partitioned into two closed same sub-domains. The number of unknowns by the CFIE and IE-DDM is 1,928 and 2,352 respectively. A comparison of bistatic RCS computed using the IE-DDM solver and conventional CFIE is shown in Fig. 9 (a), a very good agreement is observed. A comparison of convergence using IE-DDM with Jacobi iteration and with Gauss-Seidel iteration is also shown in Fig. 9 (b). Obviously, Gauss-Seidel iteration has better convergence than Jacobi iteration due to it updating the currents in each sub-domain in real time.

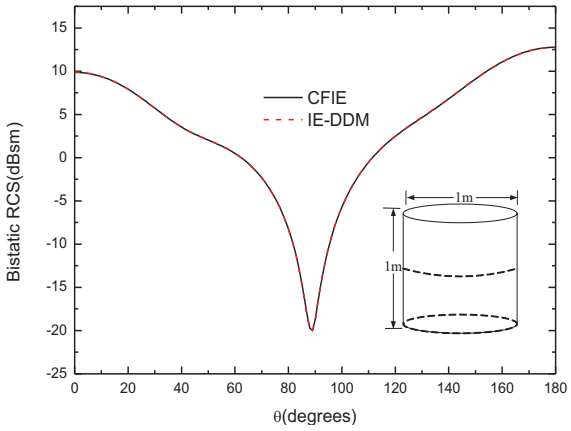

(a)

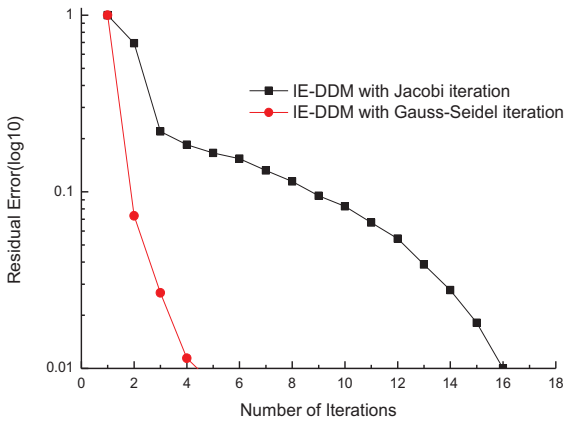

(b)

Fig. 9. (a) Bistatic RCS for PEC cylinder, and (b) the convergence history with Jacobi iteration and Gauss-Seidel iteration.

B2. Large PEC square cylinder

The scattering of a large PEC square cylinder is investigated. The frequency is 300 MHz. It is divided into 4 same sub-domains along long axial

direction. The number of unknowns by the MLFMA and IE-DDM-MLFMA is 386,400, 393,600 respectively. The incident wave, is polarized in the θ direction, with the incident angles $\theta^i = 90^\circ$ and $\varphi^i = 0^\circ$. The bistatic RCS at $\theta^s = [0^\circ, 180^\circ]$ and $\varphi^s = 0^\circ$ is shown in Fig. 10. In addition, the computational statistics on the MLFMA and IE-DDM-MLFMA is also listed in Table 1. The filling time for impedance matrix by the MLFMA and IE-DDM-BoT is 4,669, 1,290 seconds respectively. For this large PEC square cylinder, only 5 outer iterations are required to achieve the convergence threshold of 0.01. The total solution time by the MLFMA is 10,127 seconds, but the one by IE-DDM-BoT is only 5,941 seconds.

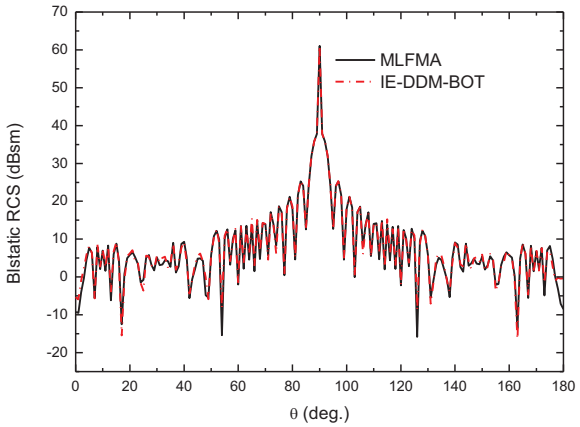

Fig. 10. Bistatic RCS for PEC square cylinder: four same sub-domains divided.

Table 1: The computational statistics using IE-DDM-MLFMA and MLFMA for large PEC square cylinder

Methods	Unknowns	Time For Filling Zmn(near) (s)	Total Solution Time (s)	Memory (MB)	Niter
MLFMA	386,400	4,669	10,127	2,032	29
IE-DDM-BoT	393,600	1,290	5,941	1,130	5

Although the IE-DDM-BoT requires more unknowns compared with the MLFMA, it reduces total CPU time and storage requirement greatly, as shown in Table 1. This is because only a few outer iterations are required by the IE-DDM-BoT, and hybrid local/global MLFMA framework can attain efficient matrix-vector multiplication in sub-domains and between sub-domains based on the feature of translational invariance of BoT.

B3. Stability investigation of IE-DDM in case of many sub-domains

Here, we use IE-DDM-MLFMA with 10, 20, 30 same sub-domains to solve three PEC circular cylinders with length of 10 m, 20 m, 30 m respectively, in order to investigate the stability of the IE-DDM-MLFMA when dividing many sub-domains. The size of sub-domain is fixed as length of 1.0 m, radius of 1.0 m. The frequency is 300 MHz. The number of unknowns by the IE-DDM-MLFMA with 10, 20, 30 sub-domains is 40,122, 83,664, and 119,814 respectively. Bistatic RCS in horizontal polarization is computed. The convergence history of IE-DDM-MLFMA for cylinders with 10, 20, 30 sub-domains is shown in Fig. 11. From Fig. 11, it is shown that the IE-DDM-MLFMA has a good convergence even for the case of 30 sub-domains.

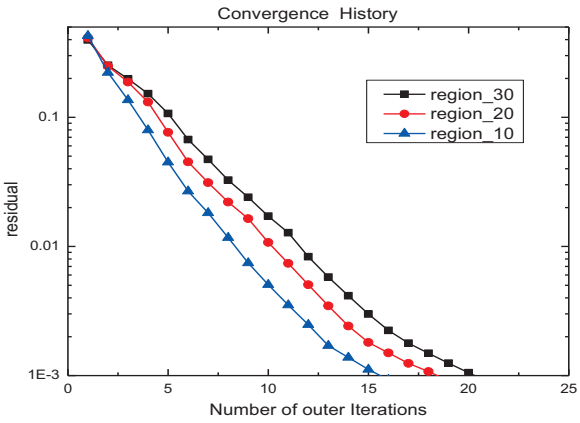

Fig. 11. The convergence history of IE-DDM-MLFMA for PEC cylinders, 10, 20, 30 same sub-domains divided.

The result of PEC cylinder with length of 20 m and radius of 1 m when dividing 20 sub-domains is shown in Fig. 12. Bistatic RCS in horizontal polarization is computed. A good agreement

between the results by the IE-DDM-MLFMA and the one by the MLFMA is also achieved, from Fig. 12. This example shows the present method using many sub-domains can still attain stable and accurate solution of large BoT.

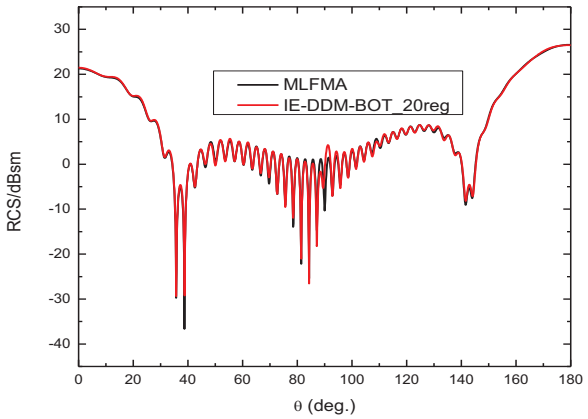

Fig. 12. Bistatic RCS for cylinder by IE-DDM-MLFMA, 20 same sub-domains divided.

VI. CONCLUSIONS

In this paper, hybrid IE-DDM-MLFMA with Gaussian-Seidel iterative technique is proposed for fast solution of PEC BoT. By updating the current in sub-domains in real time, fast convergence of outer iterations is realized.

A hybrid local/global MLFMA framework is developed for efficient implementation of fast matrix-vector multiplication in and between sub-domains. By utilizing the feature of translational invariance of BoT, the self-impedance matrix in each sub-domain is calculated only once. Compared with the traditional MLFMA, the main advantage of the present method is a reduction in storage requirements and solving time. Numerical results prove the present method is very efficient for scattering from PEC BoT.

ACKNOWLEDGMENT

Thanks to National Excellent Youth Foundation (NSFC No. 6142500243) and NSFC under Grant 61271033, the Programme of Introducing Talents of Discipline to Universities under Grant b07046.

REFERENCES

[1] L. N. Medgyesi-Mitschang and J. M. Putnam, "Scattering from finite bodies of translation: plates, curved surfaces, and noncircular cylinders," *IEEE Tran. Antennas Propagat*., vol. AP-31, no. 6, pp. 847-852, November 1983.

[2] G. Davis, "Electromagnetic calculations for large bodies of translation," *IEEE International Symposium on Antennas and Propagation*, June 18-23, 1995.

[3] L. N. Medgyesi-Mitschg and J. M. Putnam, "Formulation for wire radiators on bodies of translation with and without end caps," *IEEE Trans, Antennas Propagat*., vol. AP-31, no. 6, pp. 853-862, November 1983.

[4] J. M. Song, C. C. Lu, and W. C. Chew, "Multilevel fast multipole algorithm for electromagnetic scattering by large complex objects," *IEEE Trans. Antennas Propagat*., vol. 45, no. 10, pp. 1488-1493, October 1997.

[5] R. Xi, H. Jun, and N. Z. Ping, "Solving scattering from multiple conducting objects by hybrid multi-level fast multipole algorithm with generalized forward-and-backward method," *Electromagnetics*, 28:572-581, 2008.

[6] Z. Peng, X. C. Wang, and J. F. Lee, "Integral equation based domain decomposition method for solving electromagnetic wave scattering from non-penetrable objects," *IEEE Trans. Antenna Propagat*., vol. 59, no. 9, pp. 3328 -3338, September 2011.

[7] L. N. Medgyesi-Mitschang, J. M. Putnam, and M. B. Gedera, "Generalized method of moments for three-dimensional penetrable scatterers," *J. Opt. Soc. Am. A*, vol. 11, 1383-1398, April 1994.

[8] B. M. Kolundzija, "Electromagnetic modelling of composite metallic and dielectric structures," *IEEE Trans. on Microwave Theory and Techniques*, vol. 47, no. 7, 1021-1032, July 1999.

[9] X. Claeys and R. Hiptmair, ''Electromagnetic scattering at composite objects: a novel multi-trace boundary integral formulation,'' *ETH Zurich*, *Tech. Rep. 2011/58, Seminar for Applied Mathematics*, Zurich, Switzerland, 2011.

[10] Z. Peng, K. H. Lee, and J. F. Lee, ''Computations of electromagnetic wave scattering from penetrable composite targets using a surface integral equation method with multiple traces,'' *IEEE Trans. Antennas Propag*., vol. 61, no. 1, pp. 256-169, January 2013.

[11] S. M. Rao, D. R. Wilton, and A. W. Glisson, "Electromagnetic scattering by surfaces of arbitrary shape," *IEEE Trans. Antennas Propag*., vol. AP-30, pp. 409-418, May 1982.

[12] H. Jun, N. Zai-ping, et al., "Multilevel fast multipole algorithm for solving scattering from 3-D electrically large object," *Chinese Journal of Radio Science*, pp. 509-514, May 2004.

Jiang Ming was born in Anhui, China, in 1985. He received the B.S. degree in Electronic and Information Engineering from Anhui University in 2009. He is presently working on his Ph.D. degree in Electromagnetic Field and Microwave Technique with the Department of Microwave Engineering, at the University of Electronic Science and Technology of China (UESTC). His research interests include numerical methods in computational electromagnetic, electromagnetic scattering and radiation.

Jun Hu received the B.S., M.S., and Ph.D. degrees in Electromagnetic Feld and Microwave Technique from the University of Electronic Science and Technology of China (UESTC), Chengdu, in 1995, 1998, and 2000, respectively.

During 2001, he was with the Center of Wireless Communication in the City University of Hong Kong, Kowloon, as a Research Assistant. During March to August in 2010, he was Visiting Scholar in the ElectroScience Laboratory of Department of ECE of the Ohio State University. He was Visiting Professor of City University of Hong Kong during February to March in 2011. He is currently Full Professor with the School of Electronic Engineering of UESTC, IEEE Senior Member, and Member of Applied Computational Electromagnetics Society. He also serves as Chairman of Student Activities Committee in IEEE Cheng du Section, Vice Chairman of IEEE Chengdu AP/EMC Joint Chapter. He is the author or co-author of over 200 technical papers, received 2004 Best Young Scholar Paper prize of Chinese Radio Propagation Society. His doctoral students were awarded Best Student Paper prizes in 2010 IEEE Chengdu Section, at 2011 National Conference on Antenna, at 2011 National Conference on Microwave, at 2012 IEEE International Workshop on Electromagnetics: Applications and Students' Innovation Competition in Chengdu.

His current research interests include integral equation methods in computational electromagnetics, electromagnetic scattering and radiation.

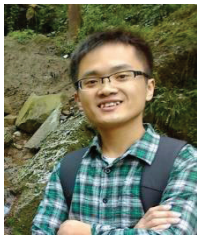

Zhao Ran received the B.S. degree in Electronic and Information Engineering from Anhui University in 2011. Since September 2011, he studied in electromagnetic field and microwave technique with the Department of Microwave Engineering, at the University of Electronic Science and Technology of China (UESTC), Chengdu, China. He is presently working on his Ph.D. degree in the same department.

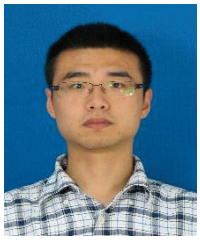

Wei Xiang received the B.E. degree in Biomedical Engineering from the University of Electronic Science and Technology of China (UESTC), Chengdu in 2011. Since September 2011, he studied in electromagnetic field and microwave technique with the Department of Microwave Engineering at UESTC. His research interests include integral equation methods in computational electromagnetics, electromagnetic scattering and radiation.

Zaiping Nie was born in Xi'an, China, in 1946. He received the B.S. degree in Radio Engineering and the M.S. degree in Electromagnetic Field and Microwave Technology from the Chengdu Institute of Radio Engineering (now UESTC: University of Electronic Science and Technology of China), Chengdu, China, in 1968 and 1981, respectively. From 1987 to 1989, he was a Visiting Scholar with the Electromagnetics Laboratory, University of Illinois, Urbana. Currently, he is a Professor with the Department of Microwave Engineering, University of Electronic Science and Technology of China, Chengdu, also IEEE Fellow. He has published more than 300 journal papers. His research interests include antenna theory and techniques, fields and waves in inhomogeneous media, computational electromagnetics, electromagnetic scattering and inverse scattering, new techniques for antenna in mobile communications, transient electromagnetic theory and applications.